Optical bistability based on an analog of electromagnetically induced transparency in plasmonic waveguide-coupled resonators

Yudong Cui* and Chao Zeng

State Key Laboratory of Transient Optics and Photonics, Xi'an Institute of Optics and Precision Mechanics, Chinese Academy of Sciences, Xi'an 710119, China

*Corresponding author: cuiyudong@opt.cn

Received 29 August 2012; revised 28 September 2012; accepted 28 September 2012; posted 2 October 2012 (Doc. ID 175216); published 23 October 2012

We have investigated numerically an optical bistability effect based on an analog of electromagnetically induced transparency (EIT) in a nanoscale plasmonic waveguide-coupled resonator system. The system consists of a metal-insulator-metal waveguide side-coupled with a slot cavity and a nanodisk cavity containing Kerr nonlinear material. By finite-difference time-domain simulations, the EIT-like spectral peak has a redshift with an increase of the dielectric constant of the nanodisk cavity. More importantly, we have achieved an optical bistability with threshold intensity about three times lower than that of recent literature [Appl. Opt. **50**, 5287 (2011)]. The results show that our plasmonic structure can find more excellent application in highly integrated optical circuits, especially all-optical switching.

OCIS codes: 240.6680, 190.1450, 140.4780.

1. Introduction

Light waves trapped on metal dielectric interfaces and coupled to propagating free electron oscillations in the metals, known as surface plasmons (SPs), are assumed to have the most potential for realization and minimization of integrated optical devices and circuits because they can effectively manipulate light at nanoscale [1,2]. Recently, more and more attention is drawn to the design of SP elements due to the capability of overcoming the diffraction limit as well as local field enhancement [1–4]. In recent years, great numbers of SP devices have been proposed and investigated numerically and experimentally [5–27]. For example, Lu *et al.* proposed some plasmonic configurations for the excellent performance of nanoscale wavelength demultiplexers [5–9]. Wang *et al.* investigated the slow light and rainbow trapping effects of the SP waves in grating waveguide systems [10,11]. And some other SP elements include Bragg reflectors [12–15], plasmonic nanosensors [16,17], filters [18,19], splitters [20–22], all-optical switching [23,24], amplifiers [25], and perfect absorbers [26,27]. As an important SP structure, metal-insulator-metal (MIM) waveguide is regarded as one of the most promising platforms for design of nanoscale photonic components because of their strong confinement of light and acceptable SP propagation length [8,16]. Recently, coupled resonators based on MIM waveguides have been widely investigated and found that they can realize the excellent manipulation of light [4–11]. Moreover, waveguide-coupled resonators possess strong field enhancement, which can promote the nonlinear effect in SP nanostructures. Optical bistability is a nonlinear optical effect that can provide light control in many respects, including all-optical information processing, and it

1559-128X/12/317482-05$15.00/0

should be considered prior to the fabrication of all-optical switching [23,28]. Recently, the optical bistability effect has been studied in many nanoscale plasmonic configurations [23,28–30]. For instance, Wang *et al.* observed an obvious optical bistability in MIM waveguide by introducing a Kerr nonlinear material into the nanodisk resonator [28]. Electromagnetically induced transparency (EIT) is a quantum effect in atomic systems which occurs due to the destructive interference of the excitation pathways to the atomic upper level [31,32]. Theoretical analysis and experimental observations demonstrate that a novel phenomenon analogous to EIT can occur in the coupled optical resonator systems owing to the coherent interference of coupled resonators [31–37]. Quite recently, Lu *et al.* reported an EIT-like resonance effect in a waveguide-coupled resonator system [31]. Could the EIT-like resonances be utilized to effectively realize the optical bistability in plasmonic nanostructures?

In this paper, we investigate numerically the transmission properties in a novel plasmonic nanostructure, which is composed of a MIM waveguide side-coupled with a slot cavity and a nanodisk resonator containing a Kerr nonlinear medium. By the finite-difference time-domain (FDTD) simulations, we obtain an excellent EIT-like resonance effect, which is employed to realize the optical bistability. It is found that the threshold intensity of the optical bistability is three times lower than the results in [28]. The results may find more applications in highly integrated optical devices, such as all-optical switching.

2. Simulation Model

Figure 1 illustrates the schematic of the plasmonic structure, which consists of a MIM waveguide with a slot cavity and a nanodisk resonator. When a TM-polarized incident light is coupled into the MIM structure, the SP waves will be excited and confined in the dielectric waveguide [12]. The dielectric in the waveguide is set as air with refractive index of 1. The nanodisk resonator is filled with a Kerr nonlinear medium. The metal is assumed to be sliver, whose frequency-dependent relative permittivity can be described by the Drude model [15,37],

$$\varepsilon_m(\omega) = \varepsilon_\infty - \frac{\omega_p^2}{\omega(\omega + i\gamma)}. \tag{1}$$

Here, ε_∞ is the dielectric constant at the infinite frequency, ω_p stands for bulk plasma frequency of free conduction electrons, γ represents the damping frequency of the electron oscillations, and ω is the angular frequency of incident light in a vacuum. These parameters for silver can be set as $\varepsilon_\infty = 3.7$, $\gamma = 0.018$ eV, and $\omega_p = 9.1$ eV [8,15]. The widths of waveguide and slot are w, the radius of nanodisk resonator is r, and the length of slot cavity is d. g_1 (g_2) represents the coupling length between the slot cavity and waveguide (nanodisk resonator). The dielectric constant of the Kerr medium depends on the intensity of incident light, which can be described as [28,38]

$$\varepsilon_d = \varepsilon_l + \chi^{(3)}|E|^2, \tag{2}$$

where ε_l represents the dielectric constant of the Kerr material and ε_d is the linear dielectric constant. Here, ε_l is assumed as 2.25, and $\chi^{(3)}$ is the third-order nonlinear susceptibility, which is set as 1×10^{-18} m^2/V^2. The parameters of the Kerr nonlinear material are the same as that in [28]. To study the transmission characteristics, we define that P_i is the total incident power and P_t is the transmission power; then the transmission efficiency is $T = P_t/P_i$ [28]. The FDTD method is utilized to investigate the optical properties

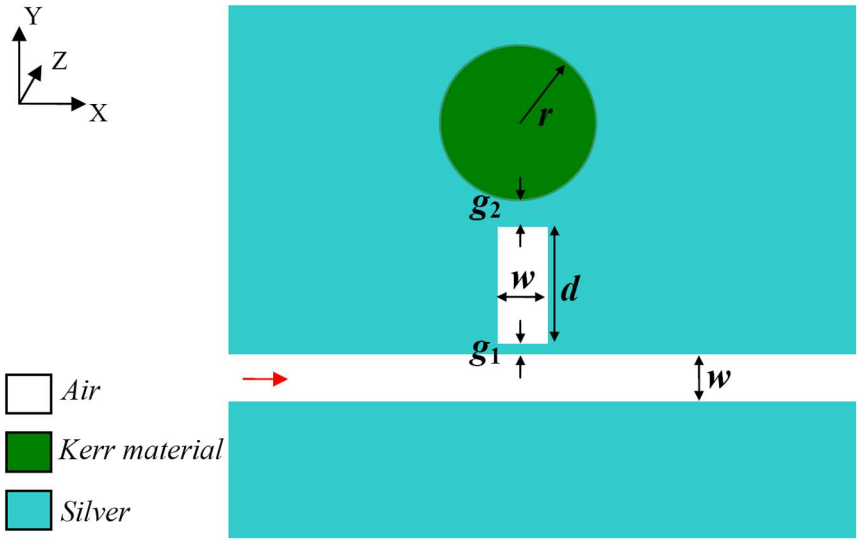

Fig. 1. (Color online) Schematic of the plasmonic structure. g_1, the coupling length between the waveguide and slot cavity; g_2, coupling length between the slot and nanodisk cavities; w, the width of the waveguide and slot cavity; r: the radius of nanodisk resonator; and d, the length of slot cavity.

in our structure [39]. The incorporation of metal dispersion into the FDTD method is achieved by using auxiliary differential equation [12,39]. In FDTD simulations, the spatial steps are set as $\Delta x = 5$ nm and $\Delta y = 5$ nm, and the temporal step is $\Delta t = \Delta x/2c$ [23]. To get accurate results, the number of time steps is set to be larger than 50,000.

3. Results and Discussion

The transmission properties of this structure are investigated numerically by the FDTD method above. The geometrical parameters of the structure are set as $r = 100$ nm, $d = 195$ nm, $w = 50$ nm, $g_1 = 10$ nm, and $g_2 = 50$ nm. Figure 2(a) shows the transmission spectra without and with a nanodisk resonator at low incident intensity, when the nonlinear term of Kerr material is not considered. The transmission exhibits a spectral dip when the nanodisk resonator is removed, which is consistent with results in [5] and [31]. The standing wave mode will be excited in the slot cavity when the incident light reaches the intrinsic resonance frequency. When the slot cavity is coupled with the nanodisk resonator, a narrow transparency peak appears in the transmitted dip. This is a typical EIT-like transmission spectrum [31,34], which occurs owing to the two possible pathways passing and bypassing the nanodisk [36]. Figure 2(b) illustrates the field distribution of $|H_z|$ at the EIT-like transparency peak of 708 nm. The light can pass through the waveguide. The

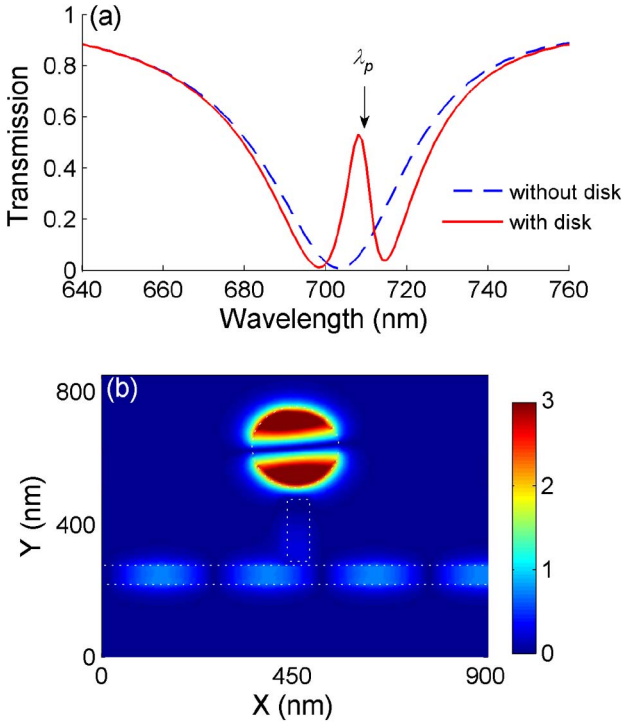

Fig. 2. (Color online) (a) Transmission spectra without (dashed curve) and with (solid curve) the nanodisk resonator. The geometrical parameters are set as $r = 100$ nm, $d = 195$ nm, $w = 50$ nm, $g_1 = 10$ nm, and $g_2 = 50$ nm. (b) Field distribution $|H_z|$ at the EIT-like resonance wavelength of 708 nm.

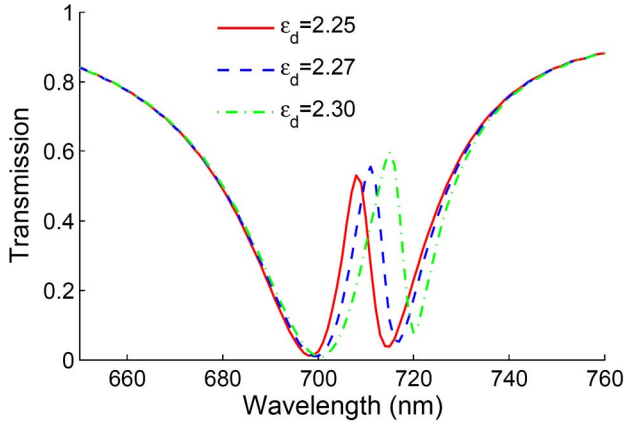

Fig. 3. (Color online) Transmission spectra with different dielectric constants in the nanodisk cavity.

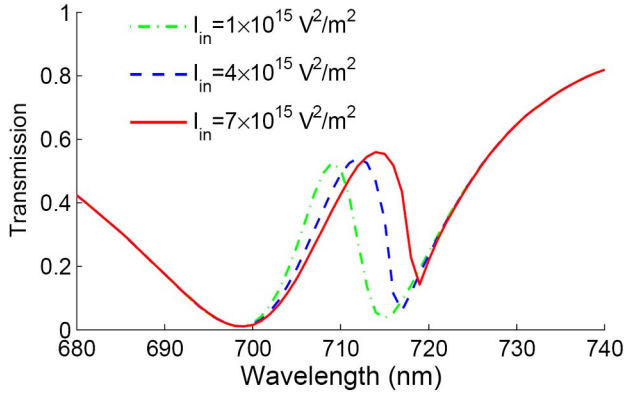

Fig. 4. (Color online) Transmission spectra with different incident intensity. The geometrical parameters are $r = 100$ nm, $d = 195$ nm, $w = 50$ nm, $g_1 = 10$ nm, and $g_2 = 50$ nm.

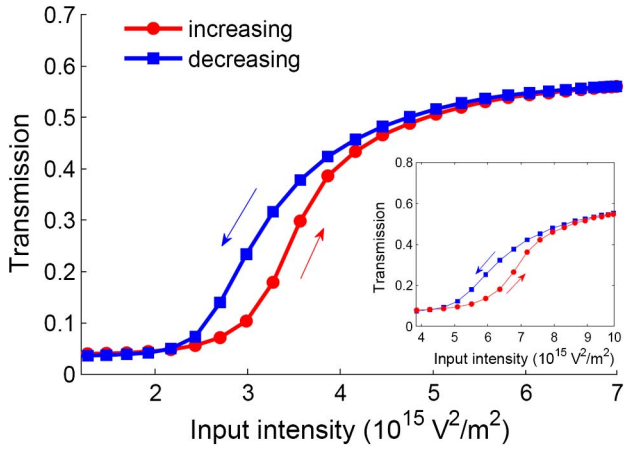

Fig. 5. (Color online) Transmission versus the increasing and decreasing intensity of incident light for the incident wavelength of 715 nm. Inset is the result with geometrical parameters of $r = 145$ nm, $d = 280$ nm, $w = 50$ nm, $g_1 = 10$ nm, and $g_2 = 40$ nm. The incident wavelength for the inset is chosen as 942 nm.

result is consistent with the spectral response in Fig. 2(a). It is worthy to note that the electromagnetic field in the slot cavity is very weak due to the destructive interference between the two pathways.

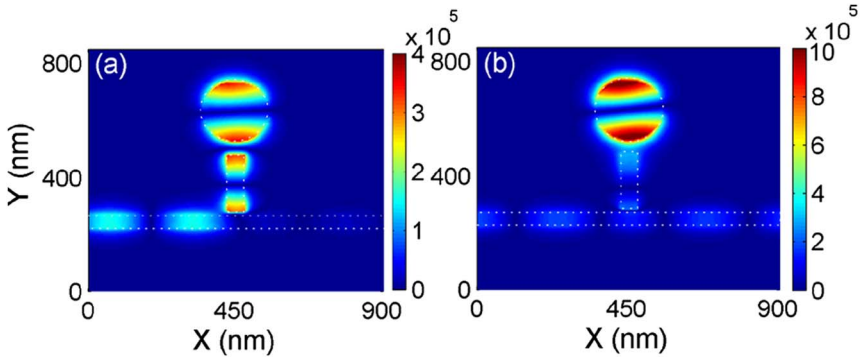

Fig. 6. (Color online) Field distributions of $|H_z|$ with the incident intensity of (a) 2×10^{15} V^2/m^2 and (b) 7×10^{15} V^2/m^2 (Media 1) for the incident wavelength of 715 nm. The geometrical parameters are $r = 100$ nm, $d = 195$ nm, $w = 50$ nm, $g_1 = 10$ nm, and $g_2 = 50$ nm.

However, the field in the nanodisk cavity is strongly enhanced due to the resonant effect, which provides a significant condition for the nonlinear effects, such as Kerr nonlinear response. Meanwhile, the resonance wavelength of the coupled nanodisk has a redshift with the increase of refractive index [2]. As can be seen in Fig. 3, the EIT-like transparency peak is sensitive to the change of the dielectric constant in the nanodisk cavity. The EIT-like resonance has a redshift for increasing the dielectric constant.

Figure 4 shows the transmission as a function of wavelength at different intensity of incident light. We can see that the transparency peak has a redshift with increasing the incident intensity. This is due to the Kerr nonlinear effect in the nanodisk cavity. With the increase of incident intensity, the electric field in the nanodisk will be strong enough to induce the obvious change of dielectric constant of the Kerr nonlinear material. The results in Fig. 4 coincide with that of Fig. 3. From Fig. 4, we can see that the transmission increases from 0.035 to 0.55 at the wavelength of 715 nm when the incident intensity changes from 2×10^{15} V^2/m^2 to 7×10^{15} V^2/m^2. The result provides a possibility for the generation of optical bistability [23,28,30]. At the fixed wavelength of 715 nm, the values of transmission efficiency are calculated by slowly increasing and decreasing incident intensities [40]. It is found that there exist two different routes for the transmission by increasing and decreasing the intensity of incident light. The optical phenomenon is assumed as the optical bistability effect [23,28]. It is noted that the output transmission can approach the stable state with high values when the intensity of incident light is about 7×10^{15} V^2/m^2. Similar to the results in [28], the bistability behavior is dependent on the geometrical parameters such as the radius of the nanodisk. Here, we adjust the parameters as $d = 280$ nm, $g_2 = 40$ nm, and $r = 145$ nm to further investigate the optical bistability effect. The fixed wavelength is set as 942 nm. The radius and operating wavelength are close to that of [28]. As shown in the inset of Fig. 5, we find that the threshold of incident intensity is about 1×10^{16} V^2/m^2, which is three times lower than that of [28]. The threshold and bistability loop are changed when the radius of the nanodisk cavity is altered. Moreover, the transmitted contrast ratio (and contrast ratio of incident intensities) of On/Off states is larger than that of [28]. The EIT-like resonance has excellent advantages for the nonlinear effect in our plasmonic nanostructure. By choosing the proper parameters, the optical bistability effect can find more excellent applications in the area of all-optical switching technology. To further confirm the transmission responses at different input intensities, the field distributions $|H_z|$ with the incident intensities of 2×10^{15} V^2/m^2 and 7×10^{15} V^2/m^2 at the wavelength of 715 nm are plotted in Fig. 6. The geometrical parameters are the same as that of Fig. 4. It is obvious that the incident light is reflected with the low input intensity in the plasmonic system, where the coupled cavity acts as a reflector [37]. When the intensity is changed to 7×10^{15} V^2/m^2, the incident light can pass through the waveguide. The induced transparency resonance is established in the nanodisk cavity due to the intensity-induced change of dielectric constant of the Kerr nonlinear material.

4. Conclusions

In this paper, the optical bistability response has been investigated numerically in a novel plasmonic resonator system which consists of a strong confined MIM waveguide with a slot cavity and a nanodisk cavity containing a Kerr nonlinear material. The plasmonic structure exhibits a typical EIT-like spectral performance due to the optical interference of the coupled resonator. By the FDTD simulations, the EIT-like spectral peak exhibits a redshift with the increase of the intensity of incident light. Meanwhile, the EIT-like resonance can realize the optical bistability behavior with a threshold three times lower than that of the conventional resonance of the coupled nanocavity reported in [28]. Our plasmonic structure may find more potential applications in highly integrated optical circuits and signal processing, especially all-optical switching.

This work was supported by the National Natural Science Foundation of China under Grants 1087-4239, 10604066, and 11204368.

References

1. W. L. Barnes, A. Dereux, and T. W. Ebbesen, "Surface plasmon subwavelength optics," Nature **424**, 824–830 (2003).
2. H. Lu, X. Liu, Y. Gong, L. Wang, and D. Mao, "Multi-channel plasmonic waveguide filters with disk-shaped nanocavities," Opt. Commun. **284**, 2613–2616 (2011).
3. G. A. Wurtz, R. Pollard, and A. V. Zayats, "Optical bistability in nonlinear surface-plasmon polaritonic crystals," Phys. Rev. Lett. **97**, 057402 (2006).
4. R. Zia, J. A. Schuller, and M. L. Brongersma, "Plasmonics: The next chip-scale technology," Mater. Today **9**, 20–27 (2006).
5. H. Lu, X. Liu, L. Wang, D. Mao, and Y. Gong, "Nanoplasmonic triple-wavelength demultiplexers in two-dimensional metallic waveguides," Appl. Phys. B **103**, 877–881 (2011).
6. G. Wang, H. Lu, X. Liu, D. Mao, and L. Duan, "Tunable multi-channel wavelength demultiplexer based on MIM plasmonic nanodisk resonators at telecommunication regime," Opt. Express **19**, 3513–3518 (2011).
7. H. Lu, X. Liu, Y. Gong, D. Mao, and L. Wang, "Enhancement of transmission efficiency of nanoplasmonic wavelength demultiplexer based on channel drop filters and reflection nanocavities," Opt. Express **19**, 12885–12890 (2011).
8. H. Lu, X. Liu, D. Mao, Y. Gong, and G. Wang, "Analysis of nanoplasmonic wavelength demultiplexing based on MIM waveguides," J. Opt. Soc. Am. B **28**, 1616–1621 (2011).
9. F. Hu, H. Yi, and Z. Zhou, "Wavelength demultiplexing structure based on arrayed plasmonic slot cavities," Opt. Lett. **36**, 1500–1502 (2011).
10. G. Wang, H. Lu, and X. Liu, "Trapping of surface plasmon waves in graded grating waveguide system," Appl. Phys. Lett. **101**, 013111 (2012).
11. G. Wang, H. Lu, and X. Liu, "Dispersionless slow light in MIM waveguide based on a plasmonic analogue of electromagnetically induced transparency," Opt. Express **20**, 20902–20907 (2012).
12. Y. Gong, L. Wang, X. Hu, X. Li, and X. Liu, "Broad-bandgap and low-sidelobe surface plasmon polariton reflector with Bragg-grating-based MIM waveguide," Opt. Express **17**, 13727–13736 (2009).
13. J. Park, H. Kim, and B. Lee, "High order plasmonic Bragg reflection in the metal-insulator-metal waveguide Bragg grating," Opt. Express **16**, 413–425 (2008).
14. B. Wang and G. P. Wang, "Plasmon Bragg reflectors and nanocavities on flat metallic surfaces," Appl. Phys. Lett. **87**, 013107 (2005).
15. Z. H. Han, E. Forsberg, and S. He, "Surface plasmon Bragg gratings formed in metal-insulator-metal waveguides," IEEE Photon. Technol. Lett. **19**, 91–93 (2007).
16. H. Lu, X. Liu, D. Mao, and G. Wang, "Plasmonic nanosensor based on Fano resonance in waveguide-coupled resonators," Opt. Lett. **37**, 3780–3782 (2012).
17. D. V. Oosten, M. Spasenovic, and L. Kuipers, "Nanohole chains for directional and localized surface plasmon excitation," Nano Lett. **10**, 286–290 (2010).
18. H. Lu, X. M. Liu, D. Mao, L. R. Wang, and Y. K. Gong, "Tunable band-pass plasmonic waveguide filters with nanodisk resonators," Opt. Express **18**, 17922–17927 (2010).
19. Y. Gong, X. Liu, and L. Wang, "High channel-count plasmonic filter with the metal-insulator-metal Fibonacci-sequence gratings," Opt. Lett. **35**, 285–287 (2010).
20. G. Veronis and S. Fan, "Bends and splitters in metal-dielectric-metal subwavelength plasmonic waveguides," Appl. Phys. Lett. **87**, 131102 (2005).
21. M. He, J. Liu, Z. Gong, Y. Luo, X. Chen, and W. Lu, "Plasmonic splitter based on the metal-insulator-metal waveguide with periodic grooves," Opt. Commun. **283**, 1784–1787 (2010).
22. G. Wang and H. Lu, "Unidirectional excitation of surface plasmon polaritons in T-shaped waveguide with nanodisk resonator," Opt. Commun. **285**, 4190–4193 (2012).
23. H. Lu, X. Liu, L. Wang, Y. Gong, and D. Mao, "Ultrafast all-optical switching in nanoplasmonic waveguide with Kerr nonlinear resonator," Opt. Express **19**, 2910–2915 (2011).
24. Y. Gong, Z. Li, J. Fu, Y. Chen, G. Wang, H. Lu, L. Wang, and X. Liu, "Highly flexible all-optical metamaterial absorption switching assisted by Kerr-nonlinear effect," Opt. Express **19**, 10193–10198 (2011).
25. I. D. Leon and P. Berini, "Amplification of long-range surface plasmons by a dipolar gain medium," Nat. Photonics **4**, 382–387 (2010).
26. Y. Gong, X. Liu, H. Lu, L. Wang, and G. Wang, "Multiple responses of TPP-assisted near-perfect absorption in metal/Fibonacci quasiperiodic photonic crystal," Opt. Express **19**, 9759–9769 (2011).
27. Y. Gong, X. Liu, H. Lu, L. Wang, and G. Wang, "Perfect absorber supported by optical Tamm states in plasmonic waveguide," Opt. Express **19**, 18393–18398 (2011).
28. G. Wang, H. Lu, X. Liu, Y. Gong, and L. Wang, "Optical bistability in metal-insulator-metal plasmonic waveguide with nanodisk resonator containing Kerr nonlinear medium," Appl. Opt. **50**, 5287–5290 (2011).
29. Y. Shen and G. Wang, "Optical bistability in metal gap waveguide nanocavities," Opt. Express **16**, 8421–8426 (2008).
30. H. Lu, X. Liu, Y. Gong, D. Mao, and L. Wang, "Optical bistability in metal-insulator-metal plasmonic Bragg waveguides with Kerr nonlinear defects," Appl. Opt. **50**, 1307–1311 (2011).
31. H. Lu, X. Liu, D. Mao, Y. Gong, and G. Wang, "Induced transparency in nanoscale plasmonic resonator systems," Opt. Lett. **36**, 3233–3235 (2011).
32. M. Fleischhauer, A. Imamoglu, and J. P. Marangos, "Electromagnetically induced transparency: optics in coherent media," Rev. Mod. Phys. **77**, 633–673 (2005).
33. R. W. Boyd and D. J. Gauthier, "Photonics: transparency on an optical chip," Nature **441**, 701–702 (2006).
34. Q. Xu, S. Sandhu, M. L. Povinelli, J. Shakya, S. Fan, and M. Lipson, "Experimental realization of an on-chip all-optical analogue to electromagnetically induced transparency," Phys. Rev. Lett. **96**, 123901 (2006).
35. X. Yang, M. Yu, D. L. Kwong, and C. W. Wong, "All-optical analog to electromagnetically induced transparency in multiple coupled photonic crystal cavities," Phys. Rev. Lett. **102**, 173902 (2009).
36. K. Totsuka, N. Kobayashi, and M. Tomita, "Slow light in coupled-resonator-induced transparency," Phys. Rev. Lett. **98**, 213904 (2007).
37. H. Lu, X. Liu, and D. Mao, "Plasmonic analog of electromagnetically induced transparency in multi-nanoresonator-coupled waveguide systems," Phys. Rev. A **85**, 053803 (2012).
38. C. Min, P. Wang, C. Chen, Y. Deng, Y. Lu, H. Ming, T. Ning, Y. Zhou, and G. Yang, "All-optical switching in subwavelength metallic grating structure containing nonlinear optical materials," Opt. Lett. **33**, 869–871 (2008).
39. A. Taflove and S. C. Hagness, *Computational Electrodynamics: The Finite-Difference Time-Domain Method*, 2nd ed. (Artech, 2000).
40. J. Porto, L. Martín-Moreno, and F. García-Vidal, "Optical bistability in subwavelength slit apertures containing nonlinear media," Phys. Rev. B **70**, 081402 (2004).